ELSEVIER

Journal of Molecular Catalysis A: Chemical 115 (1997) 339–346

JOURNAL OF MOLECULAR CATALYSIS A: CHEMICAL

Acidities of sulfate species formed on a superacid of sulfated alumina

Tien-syh Yang [a], Tsong-huei Chang [b], Chuin-tih Yeh [a,*]

[a] *Department of Chemistry, Tsing-Hua University, Hsinchu 300, Taiwan, ROC*

[b] *Department of Chemical Engineering, Ming-Hsin Institute of Technology and Commerce, Hsinfeng, Hsinchu 304, Taiwan, ROC*

Received 18 April 1996; accepted 14 June 1996

Abstract

Sulfated alumina was prepared by impregnating γ-Al_2O_3 with aqueous H_2SO_4. Various sulfate species formed in these samples depended on the concentration of H_2SO_4 ($[H_2SO_4]$). Three sulfate species, i.e., surface sulfate, multilayer sulfate and crystallized $Al_2(SO_4)_3$ could be clearly identified by the DTG peaks at ca. 950°C, 630°C and 800°C, respectively. Surface sulfates were the main sulfate species at $[H_2SO_4] \leq 0.8$ M and induced Lewis superacidic sites ($H_0 \leq -13.8$). The superacidic sites were also characterized by a NH_3-TPD peak around 400°C and showed a catalytic activity towards *n*-butane isomerization. When $[H_2SO_4] > 0.8$ M, multilayer sulfates were additionally formed, which created weaker Brønsted acid sites with a NH_3-TPD peak around 250°C and a negligible activity towards *n*-butane isomerization. Until $[H_2SO_4] > 2.4$ M, neutral crystallized $Al_2(SO_4)_3$ was formed concurrently with the surface and the multilayer sulfates.

Keywords: Sulfated alumina; Superacid; Derivative thermogravimetry (DTG); Temperature-programmed desorption of ammonia (NH_3-TPD); *n*-Butane isomerization

1. Introduction

Sulfated metal oxides (SO_4^{2-}/MO_X) are superacidic catalysts that can catalyze isomerization of paraffins [1–3], acylation of aromatics [4], dehydration of alcohols [5,6], and so on. Among these sulfated metal oxides, SO_4^{2-}/ZrO_2 has the strongest superacidity ($H_0 \leq -16.0$) and a fair activity for *n*-butane isomerization, and hence, has been studied extensively in literature [3,7–11]. However, granule forming is always a difficult procedure for the zirconia support.

Alumina was generally used as the support of industrial catalysts, because it had a high surface area and can be formed easily without a binder. Arata et al. has reported that sulfated alumina (SO_4^{2-}/Al_2O_3) had a superacidity with $H_0 \leq -14.5$ [12]. In addition, SO_4^{2-}/Al_2O_3 could be prepared from γ-Al_2O_3, which can be obtained commercially. Therefore, the easy forming and preparation of the SO_4^{2-}/Al_2O_3 with a high superacidic density attracted our attention.

Active SO_4^{2-}/Al_2O_3 was generally prepared with around 3 M concentration of H_2SO_4 [12,13]. However, most other important sulfated metal oxides (e.g., SO_4^{2-}/Fe_2O_3, TiO_2 and

* Corresponding author.

PII S1381-1169(96)00283-X

ZrO_2) had to be prepared with a 0.5 M H_2SO_4 solution [1–5]. Evidently, an optimum concentration of H_2SO_4 to prepare an active catalyst varies with the metal-oxide used. Therefore, we want to know the effect of $[H_2SO_4]$ on the formation of various sulfate species in SO_4^{2-}/Al_2O_3.

The sulfate species on sulfated metal oxides tend to decompose into gaseous SO_3 at temperatures between 500 and 1000°C [12]. Accordingly, the sulfate loading of SO_4^{2-}/MO_X has been estimated by a thermogravimetric analysis (TGA). In this study, we intend to report that derivative thermogravimetry (DTG) can distinguish various sulfate species formed in SO_4^{2-}/Al_2O_3 due to their differences in thermal stability. Furthermore, the acidities of these sulfate species were characterized by NH_3-TPD and pyridine-IR, and the induced catalytic activities were tested by the reaction of n-C_4 isomerization.

2. Experimental

2.1. Catalyst preparation

Sulfated alumina with various sulfate loadings were prepared by impregnating 1 g of commercial γ-Al_2O_3 (Merck, surface area 108 $m^2\ g^{-1}$) with 10 ml H_2SO_4 of different concentration (0.2–4.8 M). After stirring for 10 min the impregnated slurries were filtered, and subsequently dried at 110°C for 12 h. Each sample was calcined at 550°C for 3 h and stored in vials (sealed with parafilm) as testing samples for further characterizations. These samples were named as x-SO_4^{2-}/γ-Al_2O_3 (see Table 1), where x denoted the concentration of H_2SO_4 solution.

2.2. Thermogravimetric analysis (TGA / DTG)

The sulfate loading in each samples was determined gravimetrically on a thermal analysis system (Seiko TG/DTA 300). After 30 min of dehydration at 400°C, the sample temperature was linearly raised, at a rate of 10°C min^{-1}, to 1200°C in an Ar flow (100 ml min^{-1}). Pure γ-Al_2O_3 was used as a blank in the reference port to compensate the possible interference from the dehydration on the surface of γ-Al_2O_3. The sulfate loading (SL, wt%) of testing samples was estimated from the weight loss (Δm) between 400 and 1200°C in TGA profiles. The DTG profiles were obtained by differentiating the profiles of TGA.

2.3. Acidity measurement

The maximum acidic strength of testing samples was characterized by a Hammett indicator method. Detailed procedures can be found in the literature [14].

The indicators used in this article had their pK_a value ranging from -12.4 to -14.5 and the solvent used was n-heptane (Table 1).

The acidic distribution of testing sample was determined by a TPD of ammonia (NH_3-TPD) in a fixed-bed flow reactor. Each sample (0.1 g) was dehydrated by an evacuation at 300°C for 1 h before exposed to a flow of dry NH_3 gas at 100°C. After the sample was saturated with NH_3, excessive and physically adsorbed NH_3 molecules were purged away with an Ar flow at the same temperature. The NH_3-TPD was performed by raising the system temperature from

Table 1
Acidic strengths of various SO_4^{2-}/γ-Al_2O_3 samples measured by a Hammett indicator method

Samples	$H_0 \leq -12.44$ [a]	$H_0 \leq -13.75$	$H_0 \leq -14.52$
0.2-SO_4^{2-}/γ-Al_2O_3	+ [b]	+	±
0.8-SO_4^{2-}/γ-Al_2O_3	+	+	±
1.6-SO_4^{2-}/γ-Al_2O_3	+	+	±
2.4-SO_4^{2-}/Al_2O_3	+	+	−
3.6-SO_4^{2-}/Al_2O_3	+	+	−
4.8-SO_4^{2-}/γ-Al_2O_3	+	+	−

[a] Indicators used for $H_0 \leq -12.44$ is p-nitrofluorobenzene, $H_0 \leq -13.75$ is 2,4-dinitrotoluene and $H_0 \leq -14.52$ is 2,4-dinitrofluorobenzene.

[b] '+' shows the color change from the basic form (colorless) to acidic form (yellow) of the indicators, '−' does not, and '±' shows ambiguously.

100 to 600°C in the Ar flow at a rate of 30 ml min^{-1}. The evolved ammonia was trapped in a H_3BO_3/NH_4Cl solution located at the downstream of the flow and titrated with sulfamic acid using an on-line automatic pH titrator.

FT-IR spectra of adsorbed pyridine (Py) were used to distinguish the nature of acid sites (Lewis or Brønsted) on the testing samples. A Nicolet 730 infrared spectrometer was used for this measurement. In this study, the disc samples were dehydrated at 400°C for 2 h, and then cooled down to 100°C for pyridine adsorption. After pyridine adsorption, the samples were purged with He gas at 150°C to remove the weakly adsorbed pyridine.

2.4. XPS characterization

The surface composition of testing samples were measured with X-ray photoelectron spectra (XPS) using a PHI 1600 spectrometer. The vacuum of the spectrometer was better than 1×10^{-8} mbar during the spectra acquisition.

Testing samples were excited with Al Kα radiation (1486.6 eV, 15 kV, 250 W). The recorded B.E. was referred to $C(1s) = 284.8$ eV. The surface composition was estimated from the relative integral intensity (peak area) of the S(2p) and Al(2p) lines.

2.5. Catalytic test

n-Butane isomerization was carried out in a flow system with a fixed bed reactor to test the acidic activity of prepared samples. Before the reaction, each SO_4^{2-}/γ-Al_2O_3 sample was calcined in a flow of air at 550°C for 3 h. The catalytic conversion was measured at 300°C with the feed about *n*-C_4 WHSV of 1 h^{-1} and H_2/n-C_4 of 6 (molar ratio). The reaction products were analyzed with an on-line gas chromatograph using a FID detector and a 30 m long, 0.53 mm i.d. capillary column (SE™-30).

3. Results and discussion

3.1. Sulfate species assignment

Fig. 1 presents the effect of H_2SO_4 concentration ($[H_2SO_4]$) on the sulfate loading (SL) of prepared SO_4^{2-}/γ-Al_2O_3 sample. The obtained curve clearly displays three stages of SO_4^{2-} uptake. The SL increased linearly with $[H_2SO_4]$ as $[H_2SO_4] < 0.8$ M, slightly leveled off around 4–5 wt% in the $[H_2SO_4]$ range of 0.8–1.6 M and increased again after raising $[H_2SO_4]$ above 1.6 M. The increment of SL during $[H_2SO_4] <$ 0.8 M may be due to the monolayer of surface sulfate is not reached until $[H_2SO_4]$ approaches 0.8 M. Beyond monolayer, the multilayer sulfate is formed, thereby leading to a further increase of SL at $[H_2SO_4] > 1.6$ M.

Fig. 2 illustrates the DTG profiles of SO_4^{2-}/γ-Al_2O_3 samples impregnated with different $[H_2SO_4]$. The DTG results indicated that a decomposition peak around 950°C appeared while $[H_2SO_4] \leq 0.8$ M (Fig. 2b and c). In this stage, the peak width became broadened toward lower temperatures with an increasing $[H_2SO_4]$. As $[H_2SO_4]$ increased over 0.8 M, a second peak appeared around 630°C. The intensity of

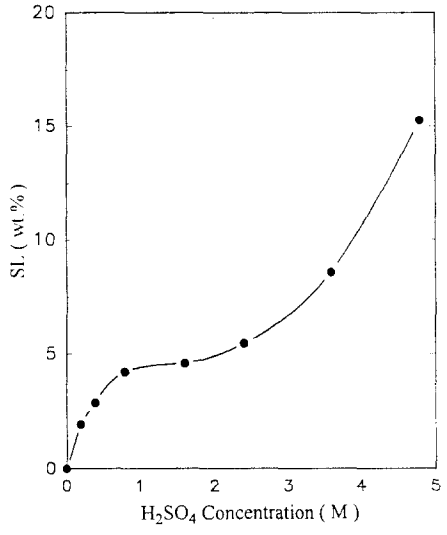

Fig. 1. Effects of $[H_2SO_4]$ on the sulfate loading (SL) of SO_4^{2-}/γ-Al_2O_3 samples.

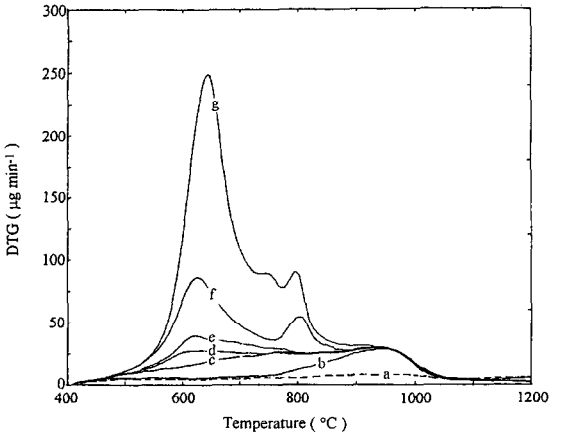

Fig. 2. DTG profiles of (a) γ-Al_2O_3 and SO_4^{2-}/γ-Al_2O_3 samples impregnated with $[H_2SO_4]$ (b) 0.2 M, (c) 0.8 M, (d) 1.6 M, (e) 2.4 M, (f) 3.6 M and (g) 4.8 M.

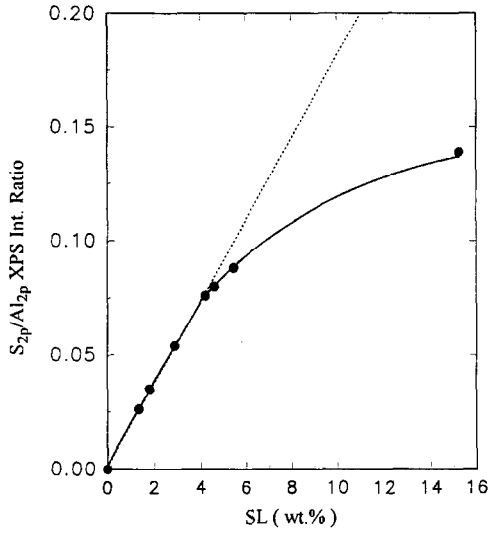

Fig. 3. Variation of S(2p)/Al(2p) XPS intensity ratio with SL for SO_4^{2-}/γ-Al_2O_3 samples.

this peak increased successively with increasing $[H_2SO_4]$ (Fig. 2d–g). As $[H_2SO_4] > 2.4$ M, a third peak at ca. 800°C appeared. The peak temperature is similar to the decomposition temperature of pure $Al_2(S0_4)_3$ [15]. From the comparison between Figs. 1 and 2, it was indicated that the large increment of sulfate loading at $[H_2SO_4] > 1.6$ M (Fig. 1) resulted from the formations of two sulfate species, as illustrated by the appearances of two DTG peaks around 630 and 800°C (Fig. 2).

In this study, the S(2p)/Al(2p) XPS integral intensity ratio was used to assess the dispersion of SO_4^{2-} anions over the alumina surface. As depicted in Fig. 3, the ratio increased linearly with the SL up to 4.2 wt% (when $[H_2SO_4] = 0.8$ M). Beyond this sulfate loading, the ratio departed from the linear relationship and became concave down. The departure from the linearship indicated a formation of multiayer sulfates.

Comparing the XPS results with the DTG profiles (Fig. 2), the DTG peak at 630°C should be contributed by the multilayer sulfates, whereas the broad peak around 950°C results from the surface sulfates. However, the interaction strengths of the surface sulfates with γ-Al_2O_3 are different. It is indicated from profiles in Fig. 2b and c that the surface sulfates initially formed have a stronger interaction than those deposit at latter times, hence, the peak around 950°C became broadened towards lower temperatures with an increasing $[H_2SO_4]$.

Fig. 4 compares XRD patterns obtained from the γ-Al_2O_3, samples of SO_4^{2-}/γ-Al_2O_3 and the $Al_2(S0_4)_3$. Besides the pattern of γ-Al_2O_3 (Fig. 4a), the SO_4^{2-}/γ-Al_2O_3 samples impregnated with $[H_2SO_4] \leq 2.4$ M (Fig. 4b and c) do not exhibit any additional diffraction peaks. When $[H_2SO_4] > 2.4$ M (Fig. 4d and e), a

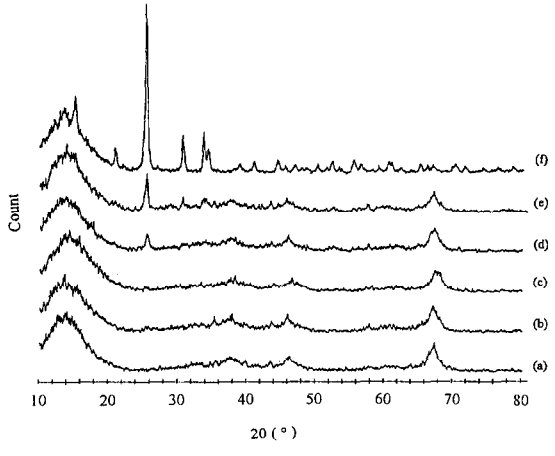

Fig. 4. XRD patterns of (a) γ-Al_2O_3 and SO_4^{2-}/γ-Al_2O_3 samples impregnated with $[H_2SO_4]$ (b) 1.6 M, (c) 2.4 M, (d) 3.6 M, (e) 4.8 M and (f) $Al_2(SO_4)_3$.

Table 2
Characterization of sulfate species on SO_4^{2-}/γ-Al_2O_3

Sulfate species	$[H_2SO_4]$ (M)	DTG (°C)	NH_3-TPD (°C)	Py-IR
Surface sulfate	≤ 0.8	950	400 and 220	Lewis acid
Multiayer sulfate	> 0.8	630	220	Brønsted acid
$Al_2(SO_4)_3$	> 2.4	800	–	–

characteristic diffraction peak ($2\theta = 26°$) of crystallized $Al_2(S0_4)_3$ (Fig. 4f) appeared. A comparison of the XRD results with the DTG profiles reveals that the DTG peak at 800°C (produced at $[H_2SO_4] > 2.4$ M) definitely comes from crystallized $Al_2(S0_4)_3$. The DTG peak at 950°C does not show any XRD signals because it belongs to surface sulfate. Whereas, the DTG peak at 630°C should be an amorphous multilayer sulfate.

Accordingly, three sulfate species formed in SO_4^{2-}/γ-Al_2O_3 samples can be distinguished by the DTG peaks. The peaks at 950°C, 630°C and 800°C are assigned to the decomposition of surface sulfate, amorphous multilayer sulfate and crystallized $Al_2(S0_4)_3$ respectively. The formations of these sulfate species depend on the $[H_2SO_4]$ of impregnating solution (Table 2). The surface sulfate was the dominant sulfate species at $[H_2SO_4] \leq 0.8$ M. When $[H_2SO_4] >$ 0.8 M, the multilayer sulfate was additionally formed. Until $[H_2SO_4] > 2.4$ M, crystallized $Al_2(SO_4)_3$ was formed concurrently with the surface and multilayer sulfates.

3.2. Acidity measurement

Acidity is the most important catalytic function for sulfated metal oxides. Therefore, this section attempts more thoroughly to understand the acidic properties, including acidic distribution and nature, caused by three sulfate species distinguished in the previous section.

Fig. 5 displays the NH_3-TPD profiles for γ-Al_2O_3 and the SO_4^{2-}/γ-Al_2O_3 samples. The NH_3-TPD profile of γ-Al_2O_3 exhibited a broad peak around 200°C (Fig. 5a). After the surface sulfates were impregnated at $[H_2SO_4] \leq 0.8$ M, two NH_3-desorption peaks were observed (Fig. 5b and c): one appeared around 400°C and the other was located around 220°C. Both peaks increased with $[H_2SO_4]$. Therefore, the surface sulfates could induce two kinds of acid site: a strong acid sites characterized by the peak around 400°C and a weak acid sites characterized by the peak around 220°C.

As the $[H_2SO_4]$ was increased over 0.8 M, the intensity of 400°C peak remained unchanged. The intensity of 220°C peak, however, increased progressively as the multilayer sulfates were formed (Fig. 5d–f). Accordingly, the multilayer sulfates created mainly the weak acid sites. It should be mentioned here that pure $Al_2(SO_4)_3$ after calcining at 550°C had no NH_3-TPD peak (not shown) because it had no acidity with $H_0 \leq +0.8$ [16].

Corma et al. [11] have used the NH_3-TPD to characterize the acidity of the SO_4^{2-}/ZrO_2 superacid. A sharp peak at 542°C (815 K) was found to characterize the superacidic sites. We observed a peak around 400°C from our sulfated alumina. Evidently, the superacidity of SO_4^{2-}/γ-Al_2O_3 in our study is weaker than

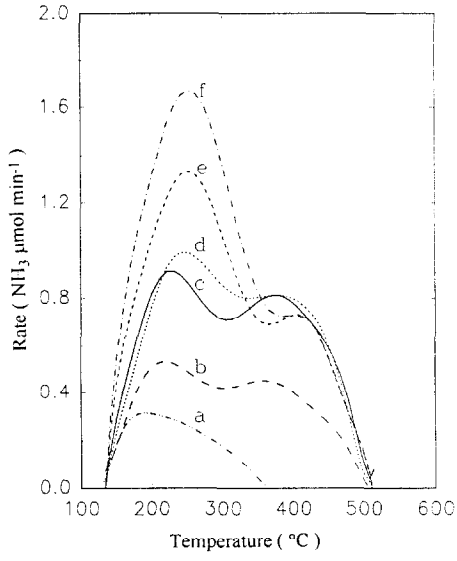

Fig. 5. NH_3-TPD profiles of (a) γ-Al_2O_3 and SO_4^{2-}/γ-Al_2O_3 samples impregnated with $[H_2SO_4]$ (b) 0.2 M, (c) 0.8 M, (d) 1.6 M, (e) 3.6 M and (f) 4.8 M.

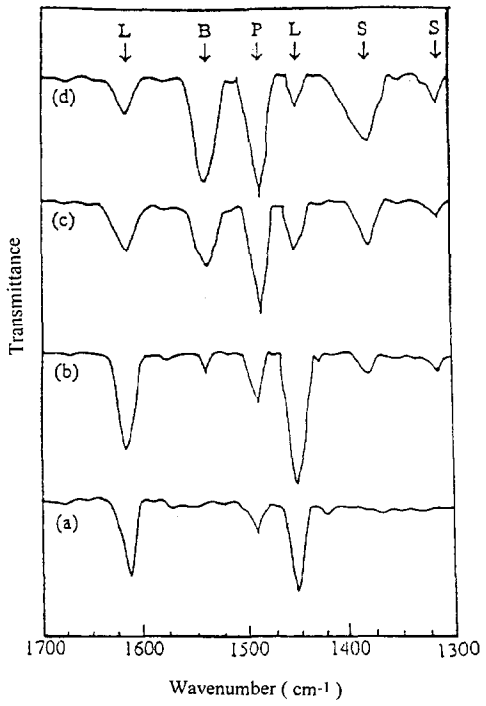

Fig. 6. FT-IR spectra of pyridine adsorbed on (a) γ-Al_2O_3 and SO_4^{2-}/γ-Al_2O_3 samples impregnated with [H_2SO_4] (b) 0.8 M, (c) 1.6 M, (d) 3.6 M. B: Py on Brønsted acid sites; L: Py on Lewis acid sites; P: adsorbed Py; S: sulfates on γ-Al_2O_3.

their SO_4^{2-}/ZrO_2. Hammett indicator tests confirmed that our SO_4^{2-}/γ-Al_2O_3 samples had a weaker superacidity ($H_0 \leq -13.8$, Table 1) than SO_4^{2-}/ZrO_2 ($H_0 \leq -16.0$) [3].

Fig. 6 displays the Py-IR spectra of γ-Al_2O_3 and various SO_4^{2-}/γ-Al_2O_3 samples. The segment of Py-IR spectra between 1700 and 1300 cm^{-1} have been well characterized in literature [17]. Both peaks at 1610 and 1450 cm^{-1} are assigned to Py adsorbed on Lewis acid site (assigned as L peaks in Fig. 6); the peak at 1540 cm^{-1} is characteristic of Py adsorbed on Brønsted acid site (B peak); A peak at 1490 cm^{-1} appears commonly for Py adsorbed on either Lewis or Brønsted acid sites (P peak). The results showed only Lewis acid sites were observed on pure γ-Al_2O_3 dehydrated at 400°C (Fig. 6a). When only surface sulfates were impregnated onto γ-Al_2O_3 at [H_2SO_4] = 0.8 M, the Lewis acid sites increased and a tiny Brønsted acid sites appeared (Fig. 6b). That is, the surface sulfates mainly induced the additional Lewis acid sites. When the multilayer sulfates were formed at [H_2SO_4] > 0.8 M, the Brønsted acid sites increased (Fig. 6c and d). Evidently, the multilayer sulfates created the Brønsted acid sites.

In addition to the L, B and P peaks, two other peaks are found in the segment between 1400 and 1300 cm^{-1} from the Py-IR spectra of sulfated samples (Fig. 6b–d). The peak at 1380 cm^{-1} is a characteristic peak of the sulfate on metal oxide [18,19], while the peak at 1315 cm^{-1} represents sulfate ions interacted with pyridine [20].

3.3. Catalytic activity of n-butane isomerization

n-C_4 isomerization can be catalyzed by solid superacids such as SO_4^{2-}/ZrO_2 and H-mordenite [21,22]. Three different paths have been proposed on the interaction of n-C_4 with the solid superacids. On superacidic Lewis acid sites (on SO_4^{2-}/ZrO_2), n-C_4 could isomerize directly to i-C_4 through a monomolecular carbenium-ion mechanism [22],

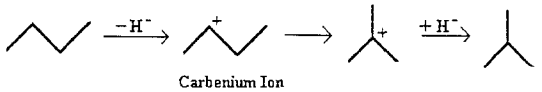

(1)

On superacidic Brønsted acid sites (on H-mordenite), i-C_4 can be produced by monomolecular carbonium-ion mechanism [22],

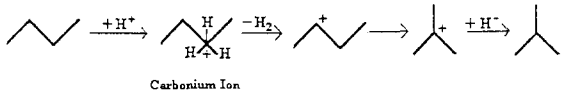

(2)

The isomerization of n-C_4^+ to i-C_4^+ needs a superacidic site to catalyze [23]. On weak acidic sites, n-C_4^+ can only deprotonate into olefin and produce C_5 and low molecular hydrocarbons

Table 3
Initial conversion [a] of n-C_4 to different products on various samples with T = 300°C, WHSV = 1 h^{-1}, H_2/n-C_4 (molar ratio) = 6

Samples	C_3^- [b]	C_3	i-C_4	C_5	Total conversion	C_5/i-C_4	C_3/C_5
γ-Al_2O_3	0	0	0	0	0	—	—
0.8-SO_4^{2-}/γ-Al_2O_3	2.8	8.8	2.2	3.7	17.5	1.7	2.4
1.6-SO_4^{2-}/Al_2O_3	4.2	9.5	2.0	4.2	19.9	2.1	2.3
3.6-SO_4^{2-}/Al_2O_3	2.7	9.7	1.3	4.0	17.7	3.1	2.4

[a] Initial conversion is measured at 5 min time-on-stream.
[b] $C_3^- = C_1 + C_2$.

through oligomerization-cracking mechanism (bi-molecular) [24],

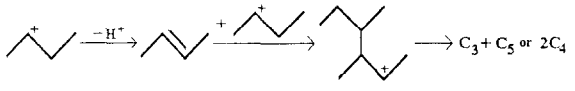

(3)

The ratio of C_5/i-C_4 in the isomerization of n-C_4 therefore depends on the acidic strength of the solid superacid. A strong superacid favors the isomerization to i-C_4 (through the path (1) or (2), with a C_5/i-C_4 ratio approaching 0) while a weak superacid favors the formation of C_5 (through the path (3), C_5/i-$C_4 > 1$).

In this study, we used n-C_4 isomerization at 300°C as a test reaction to study the acidic activities of the sulfate species characterized on SO_4^{2-}/γ-Al_2O_3. Table 3 presents the initial conversions (5 min time-on-stream) of n-C_4 at 300°C on the 0.8-, 1.6- and 3.6-SO_4^{2-}/γ-Al_2O_3 catalysts characterized previously. Pure γ-Al_2O_3 did not show any activity towards n-C_4 isomerization at 300°C. The conversion to i-C_4 on the SO_4^{2-}/γ-Al_2O_3 catalysts was low (ca. $\leq 2\%$) but significant. Among three SO_4^{2-}/γ-Al_2O_3 catalysts studied, the 0.8-SO_4^{2-}/γ-Al_2O_3 had a maximum conversion to i-C_4, although the catalyst possessed the lowest sulfate loading on comparing with the others (1.6- and 3.6-SO_4^{2-}/γ-Al_2O_3). It was therefore deduced that only surface sulfate can initiate the n-C_4 isomerization. The reduction of the i-C_4 conversion on 3.6-SO_4^{2-}/γ-Al_2O_3 was attributed to blockades of the n-C_4 diffusion to the surface sulfate by the multilayer sulfate and crystallized $Al_2(SO_4)_3$ formed at higher [H_2SO_4]. The slightly larger total conversion on 1.6-SO_4^{2-}/γ-Al_2O_3 and 3.6-SO_4^{2-}/γ-Al_2O_3 indicated the contribution of the Brønsted acid sites to the activity was insignificant due to their weak acidity. The last two columns in Table 3 list the ratios of C_5/i-C_4 and C_3/C_5. The observed C_5/i-$C_4 > 1$ indicated the isomerization of n-C_4 proceeded mainly by oligomerization-cracking mechanism (path (3)), and the observed $C_3/C_5 > 1$ suggested that a great part of C_3 can be produced by a successive oligomerization-cracking reaction [8].

4. Conclusions

DTG is a good technique for characterizing sulfate species on sulfated alumina. Three different species, i.e., surface sulfate, multilayer sulfate, and crystallized $Al_2(SO_4)_3$ can be identified from their decomposition temperatures. The surface sulfate possesses a high thermal stability, and induces a superacidity ($H_0 \leq -13.8$) that is capable of isomerizing n-C_4 to i-C_4. The multilayer sulfate exhibits a lower thermal stability and a weaker acidity. Crystallized $Al_2(SO_4)_3$ is a neutral species. The latter two species are inactive towards n-butane isomerization.

Acknowledgements

The authors would like to thank the National Science Council of the Republic of China for

financial support through the Contract No. NSC84-2113-M007-018.

References

[1] M. Hino and K. Arata, J. Chem. Soc. Chem. Commun. (1979) 1148.
[2] K. Arata and M. Hino, Shokubai 21 (1979) 217.
[3] M. Hino and K. Arata, J. Chem. Soc. Chem. Commun. (1980) 851.
[4] K. Tanabe, T. Yamaguchi, K. Akiyama, A. Mitoh, K. Iwabuchi and K. Isogai (Eds.), Proc. 8th Int. Congr. Catalysis, Vol. 5, Verlag-Chemie, Weinheim, 1984, p. 601.
[5] K. Tanabe, A. Kayo and T. Yamaguchi, J. Chem. Soc. Chem. Commun. (1981) 602.
[6] A. Kayo, T. Yamaguchi and K. Tanabe, J. Catal. 83 (1983) 99.
[7] M. Bensitel, O. Saur, J.-C. Lavalley and B.A. Morrow, Mater. Chem. Phys. 19 (1988) 147.
[8] J.C. Yori, J.C. Luy and J.M. Parera, Appl. Catal. 46 (1989) 103.
[9] F. Garin, D. Andriamasinoro, A. Abdulsamad and J. Sommer, J. Catal. 131 (1991) 199.
[10] C. Morterra, G. Cerrato, C. Emanuel and V. Bolis, J. Catal. 142 (1993) 349.
[11] A. Corma, V. Fornes, M.I. Juan-Rajadell and J.M. Lopez Nieto, Appl. Catal. A: General 116 (1994) 151.
[12] K. Arata and M. Hino, Appl. Catal. 59 (1990) 197.
[13] T. Hochmann and K. Setinek, Collect. Czech. Chem. Commun. 57 (1992) 2241.
[14] K. Tanabe, M. Misono, Y. Ono and H. Hattori (Eds.), New Solid Acids and Bases, Their Catalytic Properties, Studies in Surface Science and Catalysis, Vol. 51. (Kodansha and Elsevier, Tokyo, 1989) p. 6.
[15] H. Bassett and T.H. Goodwin, J. Chem. Soc. (1949) 2239.
[16] K. Tanabe (Ed.), Solid Acids and Bases (Kodansha, Tokyo, 1970) p. 83.
[17] E.P. Parry, J. Catal. 22 (1963) 371.
[18] A. Kayo, T. Yamaguchi and K. Tanabe, J. Catal. 83 (1983) 99.
[19] O. Saur, M. Bensitel, A.B. Mohammed Saad, J.-C. Lavalley, C.P. Tripp and B.A. Morrow, J. Catal. 99 (1986) 104.
[20] J.S. Lee, M.H. Yeom and D.S. Park, J. Catal. 126 (1990) 361.
[21] J.C. Yori, J.C. Luy and J.M. Parera, Appl. Catal. 46 (1989) 103.
[22] K.J. Chao, H.C. Wu and L.J. Leu, J. Catal. 157 (1995) 289.
[23] G.A. Olah, G.K. Surya Prakash and J. Sommer (Eds.), Superacids (John Wiley and Sons, New York, 1985) p. 254.
[24] N.N. Krupina, A.L. Proskurnin and A.Z. Dorogochinskii, React. Kinect. Catal. Lett. 32 (1986) 135.